



**US Army Corps  
of Engineers®**  
Engineer Research and  
Development Center



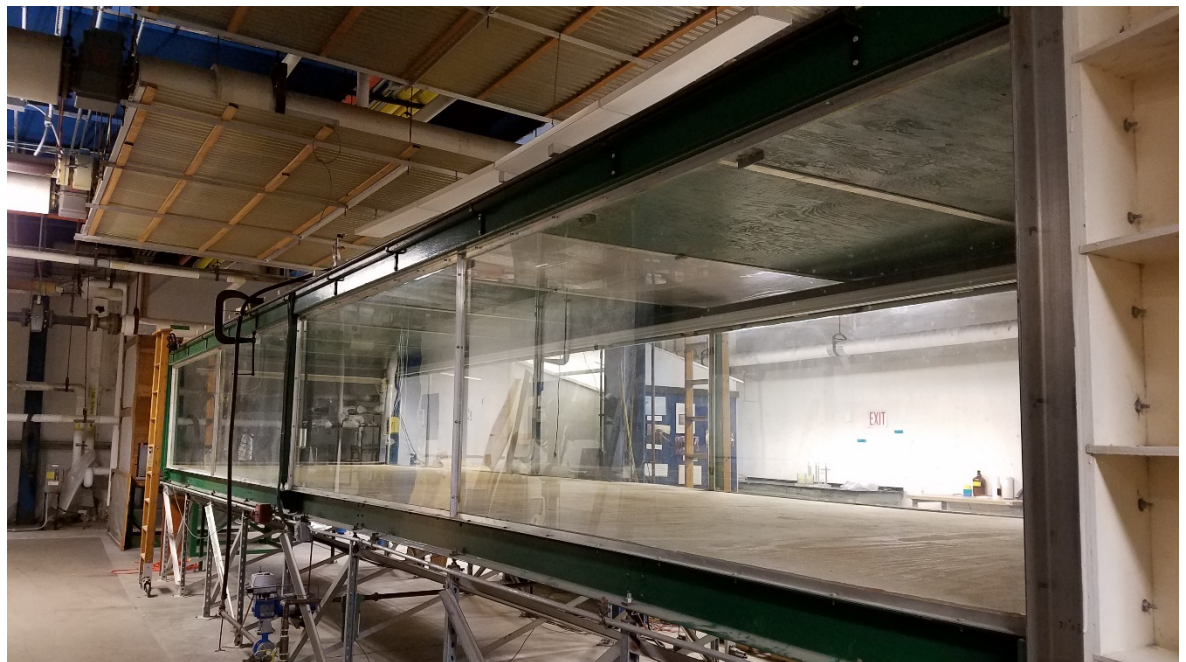
*ERDC 6.2 Geospatial Research and Engineering (GRE) ARTEMIS STO-R DUST-CLOUD*

## **CRREL Environmental Wind Tunnel**

### **Characteristics and Capabilities**

Marissa J. Torres, Alexander R. Stott, Sandra L. LeGrand,  
and Marina Reilly-Collette

May 2019



**The U.S. Army Engineer Research and Development Center (ERDC)** solves the nation's toughest engineering and environmental challenges. ERDC develops innovative solutions in civil and military engineering, geospatial sciences, water resources, and environmental sciences for the Army, the Department of Defense, civilian agencies, and our nation's public good. Find out more at [www.erdcl.usace.army.mil](http://www.erdcl.usace.army.mil).

To search for other technical reports published by ERDC, visit the ERDC online library at <http://acwc.sdp.sirsi.net/client/default>.

# **CRREL Environmental Wind Tunnel**

## **Characteristics and Capabilities**

Marissa J. Torres, Alexander R. Stott, Sandra L. LeGrand, and Marina Reilly-Collette

*U.S. Army Engineer Research and Development Center (ERDC)  
Cold Regions Research and Engineering Laboratory (CRREL)  
72 Lyme Road  
Hanover, NH 03755-1290*

## **Final Report**

Approved for public release; distribution unlimited.

Prepared for Assistant Secretary of the Army for Acquisition, Logistics, and Technology  
103 Army Pentagon  
Washington, DC 20314-1000

Under ERDC 6.2 Geospatial Research and Engineering (GRE) Army Terrestrial-  
Environmental Modeling and Intelligence System Science Technology Objec-  
tive—Research (ARTEMIS STO-R) under O53HJ0/FAN U4357509, “Dynamic  
Undisturbed Soils Testbed to Characterize Local Origins and Uncertainties of  
Dust (DUST-CLOUD)”

## Abstract

Atmospheric, or environmental, wind tunnels are ideal for basic research and applied physical modeling and for supporting the numerical model validation process. The U.S. Army Corps of Engineers, Engineer Research and Development Center (ERDC), has had an active presence in the field of research physical modeling. Between the ERDC Environmental Laboratory (EL), the Cold Regions Research and Engineering Laboratory (CRREL), and the Geotechnical and Structures Laboratory (GSL), there is one historical, three operational, and one future planned atmospheric wind tunnel. Each facility was uniquely designed to study different areas of atmospheric phenomena. This report reviews and highlights the characteristics of each facility and their target research applications. In particular, there is a desire to expand the scope of the CRREL Environmental Wind Tunnel (EWT) physical modeling capability. Expanding that capability beyond snowdrift modeling opens the door to geometrically full-scale turbulent-boundary-layer experiments on air-land and potentially air-water interfaces. Sustaining and improving internal wind-tunnel facilities is vital to the ERDC mission, promoting innovation and versatility in atmospheric physical modeling.

**DISCLAIMER:** The contents of this report are not to be used for advertising, publication, or promotional purposes. Citation of trade names does not constitute an official endorsement or approval of the use of such commercial products. All product names and trademarks cited are the property of their respective owners. The findings of this report are not to be construed as an official Department of the Army position unless so designated by other authorized documents.

**DESTROY THIS REPORT WHEN NO LONGER NEEDED. DO NOT RETURN IT TO THE ORIGINATOR.**

# Contents

<b>Abstract .....</b>	<b>ii</b>
<b>Figures and Tables.....</b>	<b>iv</b>
<b>Preface .....</b>	<b>vi</b>
<b>Acronyms and Abbreviations .....</b>	<b>vii</b>
<b>Unit Conversion Factors .....</b>	<b>viii</b>
<b>1 Introduction.....</b>	<b>1</b>
1.1 Objective.....	1
1.2 Background .....	2
1.2.1 Modeling the atmospheric boundary layer .....	3
1.2.2 Wind-tunnel configurations .....	5
1.2.3 ERDC wind-tunnel facilities .....	7
1.3 Approach .....	10
<b>2 CRREL Environmental Wind Tunnel .....</b>	<b>11</b>
2.1 Wind-tunnel structure.....	11
2.1.1 Contraction .....	11
2.1.2 Test section.....	13
2.1.3 Fan.....	16
2.1.4 Downstream trap.....	16
2.2 Instrumentation .....	18
2.2.1 Range-finding sensor .....	18
2.2.2 Hot-wire anemometer.....	20
2.2.3 Pitot tube.....	21
2.3 Velocity profile .....	22
<b>3 Recommendations for Expanded Capability .....</b>	<b>23</b>
3.1 Modular test section.....	23
3.2 Exhaust control for hazardous materials.....	23
3.3 Particle image velocimetry.....	24
3.4 Cold capabilities.....	25
<b>4 Summary.....</b>	<b>26</b>
<b>References .....</b>	<b>29</b>
<b>Appendix A: Supplemental Information .....</b>	<b>32</b>
<b>Report Documentation Page</b>	

# Figures and Tables

## Figures

1	Example diagrams of open- and closed-circuit wind-tunnel configurations: (a) a suction-fan type open-return system (NASA 2015a) and (b) a closed return system (NASA 2015b) .....	6
2	Diagram of the CRREL EWT (Haehnel et al. 1997) .....	11
3	Outer dimensions of the contraction cone of the CRREL EWT .....	12
4	Inner dimensions of the contraction cone of the CRREL EWT .....	13
5	Working section of the CRREL wind tunnel, measuring 9.75 m (32 ft) in length, 2.4 m (8 ft) wide, and 1.2 m (4 ft) tall; tempered glass siding provides an unobstructed view of the experimental setup .....	14
6	The carriage system within the test section of the CRREL EWT .....	15
7	(a) Front view of the fan (from the test section) with (b) a cross piece to reduce rotational velocity of airflow; (c) transition area between the test section and hopper, including particle trap, contraction transition, fan, and hopper .....	17
8	The downwind particle trap system located immediately after the fan of the CRREL EWT: (a) side view and (b) back view with lower back panel removed for access .....	18
9	OMRON ZS-LD350S displacement sensor located on the backside of the vertical beam of the carriage system in the test section of the EWT .....	19
10	Example of the TSI 1210 model general purpose 1-D hot-wire anemometer with dimensions shown in millimeters and inches (in parentheses); other model types can be found in TSI Incorporated (2013) .....	20
11	Example Pitot tube secured to the vertical rail of the carriage positioned in-line with the oncoming airflow .....	21
12	Vertical velocity profile in the CRREL EWT .....	22
A-1	Diagram of the CRREL Snow Drifting Wind Tunnel .....	32
A-2	Experimental vertical velocity profile in the SDWT in the presence of drifting snow particles (e.g., glass beads) .....	33
A-3	Cylindrical, open-return, push-down wind tunnel located at GSL in Vicksburg, MS .....	34
A-4	Side view diagram of the GSL wind tunnel (Graham et al. 2011) .....	34
A-5	Front view diagram of the GSL wind tunnel (Graham et al. 2011) .....	35

## Tables

1	Sample of typical flow-field capabilities and research applications achievable in aerodynamic and atmospheric wind tunnels .....	2
2	Brief summary comparing the features and characteristics of ERDC's active wind-tunnel facilities .....	9
3	The range of motion of the carriage system within the test section; X is measured from the right tunnel wall (looking down the tunnel from contraction) towards the left, Y is measured from the topmost of the	

---

	vertical rail towards the floor, and Z is measured from the end of the contraction cone towards the fan .....	15
4	Current and potential research applications achievable by ERDC wind tunnel facilities .....	27
A-1	Measured tunnel exit velocity profile at a fan control of 32 Hz .....	35

## Preface

This study was conducted for the Assistant Secretary of the Army for Acquisition, Logistics, and Technology under the U.S. Army Engineer Research and Development Center (ERDC) 6.2 Geospatial Research and Engineering (GRE) Applied Research Program's Army Terrestrial-Environmental Modeling and Intelligence System Science Technology Objective—Research (ARTEMIS STO-R) under 053HJo/FAN U4357509, “Dynamic Undisturbed Soils Testbed to Characterize Local Origins and Uncertainties of Dust (DUST-CLOUD).”

The work was performed by the Engineering Resources Branch (CEERD-RRE) and the Terrestrial and Cryospheric Sciences Branch (CEERD-RRG) of the Research and Engineering Division (CEERD-RR), ERDC Cold Regions Research and Engineering Laboratory (CRREL). At the time of publication, Dr. Caitlin Callaghan was Acting Chief, CEERD-RRE; Dr. John Weatherly was Chief, CEERD-RRG; Mr. Jared Oren was Acting Chief, CEERD-RR; and Dr. Mark L. Moran, CEERD-RZT, was the Technical Director. The Deputy Director of ERDC-CRREL was Mr. David B. Ringelberg, and the Director was Dr. Joseph L. Corriveau.

The authors would like to acknowledge those individuals who assisted in providing the materials, information, and guidance needed to complete this special report. Special thanks to Dr. Robert Haehnel and Dr. James Lever (CRREL), Mr. Paul Graham and Mr. John Furey (Geotechnical Structures Laboratory), and Ms. Cynthia Price and Mr. Paul Schroeder (Environmental Laboratory).

COL Ivan P. Beckman was Commander of ERDC, and Dr. David W. Pittman was the Director.



## Acronyms and Abbreviations

1-D	One-Dimensional
2-D	Two-Dimensional
3-D	Three-Dimensional
ABL	Atmospheric Boundary Layer
ARTEMIS	Army Terrestrial Environmental Modeling and Intelligence System
CCD	Charged Coupled Device
CRREL	Cold Regions Research and Engineering Laboratory
CTA	Constant Temperature Anemometer
DTRA	Defense Threat Reduction Agency
DUST-CLOUD	Dynamic Undisturbed Soils Testbed to Characterize Local Origins and Uncertainties of Dust
EL	Environmental Laboratory
ERDC	U.S. Army Engineer Research and Development Center
EWI	Environmental Wind Tunnel
GRE	Geospatial Research and Engineering
GSL	Geotechnical Structures Laboratory
ID	Inner Diameter
NASA	National Aeronautics and Space Administration
PIV	Particle Image Velocimetry
SDWT	Snow Drift Wind Tunnel
STO-R	Science Technology Objective—Research
VI	Virtual Instrument

## Unit Conversion Factors

Multiply	By	To Obtain
cubic feet	0.02831685	cubic meters
degrees Fahrenheit	$(F-32)/1.8$	degrees Celsius
feet	0.3048	meters
inches	0.0254	meters
microns	1.0 E-06	meters
miles per hour	0.44704	meters per second
square feet	0.09290304	square meters

# 1 Introduction

## 1.1 Objective

The U.S. Army Corps of Engineers, Engineer Research and Development Center (ERDC), has had an active presence in the field of research physical modeling in atmospheric and environmental conditions. Our researchers and customers have continued interest in modeling atmospheric phenomenon, including air emissions, aerosol dispersion, and snowdrift formation. Since the late 1980s, the ERDC Environmental Laboratory (EL), Geotechnical and Structures Laboratory (GSL), and Cold Regions Research and Engineering Laboratory (CRREL) have made significant contributions to various research areas by using their wind-tunnel facilities. Sustaining these in-house wind-tunnel facilities is vital to the ERDC mission. In addition, maintaining and expanding each facility is ultimately more cost-effective than contracting with other facilities and promotes more versatility in the modeling approach.

CRREL researchers are interested in expanding the scope of the CRREL Environmental Wind Tunnel (EWT) physical modeling capability. Historically, the EWT has been primarily used for modeling snowdrifts and suspended snow around a structure. In these studies, a large particle bed is placed upstream of the structure such that particles (usually micron-sized glass beads) are carried through the turbulent flow towards a model structure. The focus is then to study the depth, location, and rate of accumulation of the particles around a structure. Though understanding drift deposition around structures provides valuable practical application, we seek also to study the particle bed itself, extending the particle bed the full length of the tunnel. The capability to measure dust lofting and saltation for mineral-dust particles is a key component of the Army Terrestrial-Environmental Modeling and Intelligence System Science Technology Objective—Research (ARTEMIS STO-R) program's Dynamic Undisturbed Soils Testbed to Characterize Local Origins and Uncertainties of Dust (DUST-CLOUD) initiative. We require a versatile atmospheric wind tunnel capable of reproducing phenomena observed in DUST-CLOUD field experiments to validate our numerical models. This change in wind-tunnel modeling capability may open the door to geometrically full-scale turbulent-boundary-layer experiments on air-land and potentially air-water interfaces.

The objective of this document is to present a summary of the current ERDC wind-tunnel capabilities, with a particular focus on the EWT stationed at CRREL. While this report reviews and highlights the unique characteristics of each facility and their target research applications, it provides a more detailed description of the physical structure, available instrumentation, and example velocity profile over a sandy bed for the EWT. Additionally, at the end of this report, we briefly propose and discuss avenues in which to expand the scope of the EWT modeling capability, and we highlight some research areas that could be investigated with an upgraded capability.

## 1.2 Background

Since the first design and operation in Great Britain in 1871 (Baals and Corliss 1981), wind tunnels have advanced our understanding of aerodynamic and atmospheric airflow dynamics in academic, industrial, and government settings. Aerodynamic wind tunnels are primarily used in studies relating to freestream air flow, typically for flow around aircraft at high wind speeds (Mach number). A handful of these facilities have been designed for cold-weather applications, such as investigating icing accumulations on aircraft (e.g., NASA [National Aeronautics and Space Administration] Glenn Research Center, <https://www.nasa.gov/centers/glenn/home/index.html>). On the other hand, the physical simulation of the atmospheric boundary layer and studies relating to the layer's interaction with the ground is best performed in an atmospheric wind tunnel. Atmospheric, or environmental, wind tunnels are ideal for basic and applied research physical modeling and supporting the numerical model validation process. Table 1 provides a brief summary of the flow-field and research-application differences between aerodynamic and atmospheric wind tunnels.

Table 1. Sample of typical flow-field capabilities and research applications achievable in aerodynamic and atmospheric wind tunnels.

Wind tunnel	Capabilities
Aerodynamic	<ul style="list-style-type: none"><li>• Laminar, high speed flow</li><li>• Flow around objects (aircraft wing, cars, etc.)</li><li>• Flow visualization (e.g., smoke)</li></ul>
Atmospheric	<ul style="list-style-type: none"><li>• Turbulent flow to simulate environmental conditions</li><li>• Flow around objects (buildings, wind turbines, etc.)</li><li>• Flow visualization (e.g., smoke)</li><li>• Dispersion (aerosols, pollutants, etc.)</li><li>• Wind resource assessment</li></ul>

### 1.2.1 Modeling the atmospheric boundary layer

The aim of an atmospheric wind tunnel is to simulate an atmospheric boundary layer (ABL), also known as the turbulent or planetary boundary layer. To accurately perform experiments in the wind tunnel, researchers must consider several components, including the geometric scaling; flow characteristics, such as mean wind speed and turbulent structure; and for sediment transport, properly scaling the governing forces that drive particle entrainment and suspension. These components are heavily dependent on the problem of interest, thus it is vital to understand the appropriate physics that can be represented in an atmospheric wind tunnel. In this section, we will briefly discuss a few fundamentals.

The development of a properly scaled turbulent boundary layer is essential for an atmospheric wind tunnel. Conceptually, a boundary layer is a layer of fluid (e.g., water or air) moving in the immediate vicinity of a boundary (e.g., a wall or airplane wing) where viscous effects, or skin friction, are most significant. In our case, the ABL is the region where meteorological variables such as wind velocity, temperature, and humidity are influenced by the Earth's surface and is the boundary condition for the free atmosphere (Nieuwstadt and Duynkerke 1996). The thickness of the ABL is much greater than the thickness of the viscous boundary layer and is driven by both viscous and form drag (size and shape of the roughness elements, such as buildings or vegetation) effects.

Turbulence is the unsteady, irregular movement of a fluid, where laminar flow is steady and predictable flow. The turbulent structure of the flow is governed by the fluid viscosity and velocity and by the roughness of the surface over which the fluid is traveling. A common dimensionless parameter used to describe the transition from laminar to turbulent flow is the Reynolds number, which is the ratio of inertial forces to viscous forces (White 2015). The greater the velocity and rougher the surface (e.g., smooth wooden floor versus a sandy bed), the more chaotic the airflow will become and the thicker the boundary layer will be. The velocity profile should follow equation (1),

$$u_z = \frac{u_*}{\kappa} \ln \frac{z}{z_0}, \quad (1)$$

where

- $u_z$  = the velocity at height  $z$ ;
- $\kappa$  = von Karman's constant (generally accepted as 0.4); and
- $z_o$  = the aerodynamic roughness height, which helps to account for the form drag associated with the surface roughness.

Often there are two unknowns in equation (1), leaving the equation open. Closure is usually obtained experimentally by measuring  $u_z$  at several heights to determine the unknown quantities, such as  $u_*$  and  $z_o$ , for a given terrain. Here,  $u_*$  is the friction velocity, which is equal to the square root of the ratio of the surface shear stress  $\tau$  to fluid density  $\rho$ .

Meeting the conditions to successfully simulate a realistic wind field in the tunnel requires application of dimensional analysis and satisfying geometric and dynamic similarity between model and prototype scales. Careful consideration of each scaling parameter should precede every experimental setup as it is usually very difficult to satisfy all similarity parameters; scale modeling requires identification of the most relevant similarity parameters and ensuring that those are preserved between model and prototype scales (Lever and Haehnel 1995).

The concepts discussed provide a brief overview and do not reflect the detailed complexity of atmospheric wind-tunnel formulations. We recommend that the reader refer to materials cited in this document for more information (Kaimal and Finnigan 1994; Nieuwstadt and Duynkerke 1996; Munson et al. 2006; White 2015; Schlichting and Gersten 2016) and examples in research (Blocken et al. 2007; Bocciolone et al. 2008; Brown and Nickling 2008; Burri 2011; Chong et al. 2009; Clifton et al. 2006; Kanda et al. 2006; and Porte-Agel et al. 2011).

In practice, quantifying the wind field and atmospheric structure (e.g., wind speed and shear stress) within a wind tunnel is most commonly completed using an anemometer (one-, two-, or three-dimensional) placed in-line with the oncoming air flow or using flow imaging methods such as particle image velocimetry (PIV). Several types of anemometers have been developed over the years, but the most frequently used device in wind-tunnel application is the hot-wire anemometer. This device maintains a constant temperature across a thin wire and measures the amount of current

needed to maintain that temperature in the presence of air flow. Alternately, Pitot tubes measure the pressure differential between dynamic and static pressure within the tube by using a manometer and relate that difference to flow velocity. Both types of devices are ideal for small-scale measurements; however, Pitot static measurements are more amenable for providing mean wind speed as the volume of the fluid in a manometer dampens the velocity fluctuations; and pressure transducers, if used, often have low frequency response. High-frequency measurements are commonly obtained with hot-wire anemometry.

### **1.2.2 Wind-tunnel configurations**

The configuration of a wind tunnel falls into one of two categories: open-circuit or closed-circuit. Both configurations generally consist of a tube or channel-like structure and use a fan to control airflow through a test area, or test section. A wind tunnel that is open on either end and draws air from the surrounding area is an open-circuit, or open-return, tunnel (Figure 1a). This design has a low capital investment and small spatial footprint. Wind can either be pulled through or blown down the test section of the tunnel, typically referred to as a suction- or blower-type open-return wind tunnel, respectively. The wind field is generally turbulent through the tunnel; and combined with the open-air design, the open-return tunnel is ideal for environmental modeling and smoke visualization applications. Some of the drawbacks of this design are the noisy operation and high operating costs of a larger fan needed to make up for the flow momentum loss between the exit and intake.

On the other hand, a closed-circuit wind tunnel, also commonly referred to as a recirculating wind tunnel, is one that retains a fixed mass of air that is circulated in a loop through the tunnel components (Figure 1b). Recirculating wind tunnels are typically configured to have a suction-type fan pulling the air through the test section and around a series of turning vanes. The flow field tends to be superior in the test section (i.e., less turbulent, more relatively uniform flow) with the addition of turning vanes and flow straighteners. Noise and operating costs are minimized by maintaining a low net circuit pressure in the tunnel. This low pressure may cause condensation in the test section, in which case the air may need to be passed over a dryer bed prior to entering the tunnel circuit. Smoke or particle cloud visualization is more difficult in a recirculating tunnel since the materials will accumulate over time. Disadvantages of the closed-circuit design are a high capital investment, large spatial footprint, and active

cooling techniques to reduce warm running conditions. Further information about fundamental wind-tunnel design can be found in Cattafesta et al. (2010).

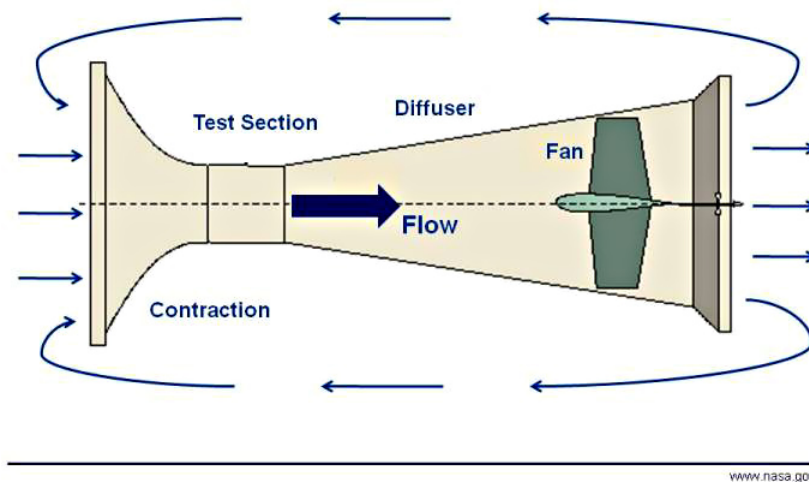
Figure 1. Example diagrams of open- and closed-circuit wind-tunnel configurations: (a) a suction-fan type open-return system (NASA 2015a) and (b) a closed return system (NASA 2015b).

(a)

National Aeronautics and Space Administration



## Open Return Wind Tunnel

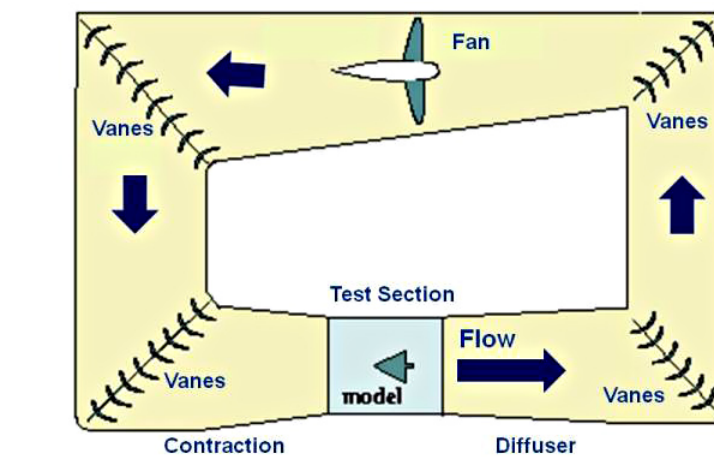


(b)

National Aeronautics and Space Administration



## Closed Return Wind Tunnel





The virtue of airflow contraction is establishing an adverse pressure gradient to suppress flow separation and to help smooth the flow going into the test section. If uniform flow is desired (aerodynamic tunnel), a short contraction length is preferred to prevent a large boundary layer from forming. In addition, a settling chamber containing a combination of fine-cell honeycombs and wire gauze screens prior to contraction will help to reduce turbulence in the test section (Bradshaw and Pankhurst 1964). These features are commonly required for blower-type and recirculating tunnels. A settling chamber is less important for an open-return suction tunnel, provided that flow is clean around the bell entrance (e.g., free of obstructions and equipment that can be a source of turbulence). Further, it is the purpose of an atmospheric wind tunnel to intentionally grow a turbulent boundary layer on the floor of the tunnel and to minimize turbulence along the wall.

The choice between the two wind-tunnel configurations ultimately depends on the type of flow field needed for the desired experiment and if the proper similitude requirements can be fulfilled within the tunnel. Modifications can be made to the flow field prior to reaching the test section as needed. For example, the size of the turbulent boundary layer (i.e., thickness or turbulence intensity) can either be increased or reduced. In practice, this technique is known as “tripping” or “smoothing” the turbulent boundary layer. Tripping the boundary layer is a method to force the wind field to become turbulent farther upstream in the tunnel. Smoothing the wind field as it enters the tunnel is a technique to reduce the turbulence intensity.

### **1.2.3 ERDC wind-tunnel facilities**

Each wind tunnel within the ERDC is designed to study a specific type of atmospheric condition. There are three operational tunnels within the ERDC, two at CRREL and one at GSL. First constructed in the early 1990s, a lysimeter wind tunnel was in operation at EL for about 20 years to study air emissions from dredged material in the Indiana Harbor Channel (Thibodeaux et al. 2008). The flow field was regulated to represent field-like (turbulent) conditions over the soil-filled lysimeter test bed. Unfortunately, it was decommissioned and dismantled approximately 5 years ago. The lysimeter tunnel was ideal for volatilization studies, sediment trapping, and controlling dust with biopolymers. Thibodeaux et al. (2008) provides details of its dimensions and characteristics.

Currently, CRREL operates two wind tunnels, one recirculating tunnel originally acquired and remodeled in 1985 (Anno 1986) and one open-return tunnel constructed in 1995 (Haehnel et al. 1997). Both wind tunnels were designed for snowdrift physical modeling. The recirculating wind tunnel was remodeled from an existing low-speed wind tunnel to the Snow Drift Wind Tunnel (SDWT). It was designed to have a logarithmic wind velocity profile, using a test bed of activated clay particles to represent snow particles. The activated clay turned out to be a visual obstacle and inhalation hazard. The tunnel was later modified in 1992 to use a test bed of glass beads (diameter on the order of microns), which required adjustment of the incident velocity profile, resulting in a log-linear profile up to 10 cm from the test bed (Haehnel et al. 1993). The perimeter of the test area is constructed from glass panels, allowing visualization of the experiment. The tunnel is equipped with two particle entrapment methods downstream of the test area: one for rolling and saltating particles and one for suspended particles. These techniques are used to measure mass transport during the course of the experiment. In recent history, the recirculating tunnel has been used to study the effects of soil moisture on the threshold conditions of entrained fine-grain sand and silt in the flow, as well as the near-bed concentrations of airborne particles (Haehnel et al. 2014).

The open-circuit suction wind tunnel at CRREL, known as the Environmental Wind Tunnel (EWT), was designed to have a fully developed turbulent boundary layer before reaching the test section. An area for optional flow straighteners was included to smooth the flow as needed. The tunnel contains similar mass flux measurement techniques as the SDWT and a working section enclosed by glass panels. In its history, the EWT has been employed in snowdrift development on a fence (Haehnel et al. 1997) and across missile hatches (Lever 2000), as well as snow drift accumulation around an elevated building (Song and Haehnel 2012). The EWT test area has also been used as an enclosed particle basin for crater evolution and particle entrainment under an impinging jet positioned at the ceiling of the test area (Haehnel 2008; Haehnel et al. 2006, 2008, 2010).

Since 2009, GSL has been operating an open-return, blower-type wind tunnel with a circular cross section for aerosol testing and particulate dispersion efforts related to the Defense Threat Reduction Agency (DTRA) mission (Graham et al. 2011, 2016). The flow field was designed to simulate atmospheric conditions, by using a turbulence grid constructed from crossing iron segments to induce turbulent flow; however, we should note

that this tunnel is not an ABL wind tunnel. Biological simulant is injected into the free stream just downwind of the turbulence grid and sampled at the outlet of the tunnel. Experimental results have calibrated and improved aerosol sampling instrumentation and techniques.

The active wind tunnels within the ERDC have unique features that are ideal for different areas of study. Table 2 reviews a few characteristics of each facility. To summarize, each tunnel is capable of generating turbulent flow conditions. The CRREL SDWT and EWT are able to explicitly recreate a turbulent boundary layer that can be modified slightly to meet the similitude requirements of individual experiments. The circular cross section of the GSL tunnel prevents a distinguished boundary layer from forming on a single plane. Each tunnel counterbalances the torsional rotation induced by the fan. The rectangular cross sections of the SDWT and EWT can accommodate multiple sensors within the working section while minimizing the effect of the instrumentation on the flow field. The GSL tunnel is primarily limited to installing instrumentation at or near the tunnel exit. The EWT is rather versatile in that the ceiling and floor panels can be removed or easily modified to accommodate other areas of interest, similar to the impinging jet studies. One can also remove the ceiling panels in the SDWT to accommodate modifications. Such features are not available in the GSL tunnel.

**Table 2. Brief summary comparing the features and characteristics of ERDC's active wind-tunnel facilities.**

Feature	GSL	CRREL EWT	CRREL SDWT
Type	Open circuit	Open circuit	Closed circuit
Fan configuration	Blow down	Suction	Suction
Cross section of test area	Circular (181.6 cm ID × 40 m [71.5 in. ID × 40 ft])	Rectangular (2.4 m × 1.2 m × 9.7 m [8 ft × 4 ft × 32 ft])	Rectangular (53 cm × 45 cm × 4 m [21 in. × 18 in. × 13 ft])
Flow	Turbulent	Turbulent	Turbulent
Velocity range (m/s [mph])	0–8 [0–18]	0–11 [0–24]	0–20 [0–45]
Research application	Particulate dispersion	Snowdrift modeling	Snowdrift modeling

Note: ID = Inner diameter

Discussed in this section are just a few high-level comparisons between the operational wind tunnels within the ERDC. This report is not an exhaustive survey of the full capability of each wind tunnel. We recommend that the reader reaches out to the authors for the point of contact of each facility for more detailed and specific information.

GSL recently acquired a recirculating wind tunnel from the Colorado School of Mines and will begin installation and experimentation in the coming months. Anticipated applications include physical modeling of land-atmospheric interactions with respect to bare soil-water evaporation to inform numerical models focused on free-fluid domains under varying atmospheric conditions. The wind tunnel will be climate-controlled using combined humidification/dehumidification and cooling/heating systems. It is not intended for Arctic purposes as the temperature ranges are expected to be between  $-4.4^{\circ}\text{C}$  ( $24^{\circ}\text{F}$ ) and  $35^{\circ}\text{C}$  ( $95^{\circ}\text{F}$ ). For more information, please reach out to the authors.

### **1.3 Approach**

In the following sections, we describe each component of the physical structure of the CRREL EWT in detail. We present both the experimental velocity profile over a sandy bed and the instrumentation currently available and commonly used in measuring wind velocity. Furthermore, we highlight potential areas of expanded capability for the EWT.

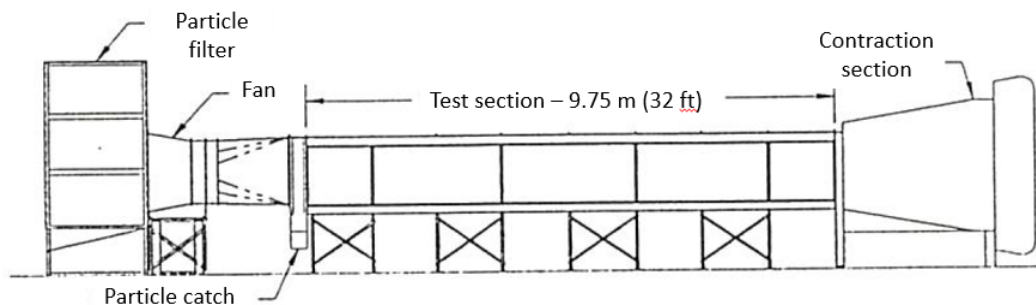
## 2 CRREL Environmental Wind Tunnel

The purpose of the CRREL EWT is to simulate the turbulent atmospheric boundary conditions that are appropriate to conduct reduced-scale physical modeling of snowdrift. Historically, there have been discrepancies in model snowdrift geometry and development rate when compared to field data due to the limitations of practical physical modeling. These issues are mentioned in Haehnel et al. (1997), and this section provides a high-level overview of each primary component of the wind-tunnel structure. For more detailed information about the materials and specifications of equipment, please contact the authors.

### 2.1 Wind-tunnel structure

The EWT is an indoor, open-circuit, rectangular tunnel composed of a contraction section, test section, suction fan, and particle traps and measures 12.3 m (60 ft) in total length (Figure 2). Air is pulled from the opening of the contraction section—located approximately 2.4 m (8 ft) from an upstream wall—through the test section, fan, and trap components and lastly expelled back into the large room. The room is located in an isolated area of the building where noise is not an issue. Vibration effects between the fan and test section are reduced by a 5 cm (2 in.) wide rubber isolator. The following sections detail each component of the wind tunnel structure.

Figure 2. Diagram of the CRREL EWT (Haehnel et al. 1997).



#### 2.1.1 Contraction

The purpose of the contraction is to accelerate and align the flow into the test section (Cattafesta et al. 2010). The flow quality in the test section is largely dependent on the size and shape of the contraction section, specifically the ratio of entrance-to-exit cross-sectional area, which ultimately

dictates the level of turbulent flow. The contraction should be small enough in length that boundary-layer growth is minimized while also being long enough to avoid large pressure gradients or separation along the wall (Cattafesta et al. 2010). Ideally, the contraction ratio should be between 6 and 12 to achieve the aforementioned conditions (Bradshaw and Pankhurst 1964).

The contraction section is constructed from two rectangular wooden frames, representing the entrance and exit sections, connected by sheets of plywood to form a curve (Figures 3 and 4). The contraction has an inflection section at the opening to accommodate flow straightening and conditioning elements as needed. A normal contraction would not have this but be a smoothly varying constriction in the downwind direction. This feature has not been used much to date but may be desirable for certain tests; Scheiman (1981) provides more information on flow straightening techniques. The total length is 3.81 m (12.5 ft). The entrance frame has a width of 3.59 m (11.81 ft) and a height of 1.98 m (6.5 ft), and the exit frame has a width of 2.4 m (7.81 ft) and a height of 1.2 m (4 ft). With an entrance cross-sectional area of 7.13 m<sup>2</sup> (76.78 ft<sup>2</sup>) and an exit cross-sectional area of 2.9 m<sup>2</sup> (31.25 ft<sup>2</sup>), the contraction ratio is approximately 2.45.

Figure 3. Outer dimensions of the contraction cone of the CRREL EWT.

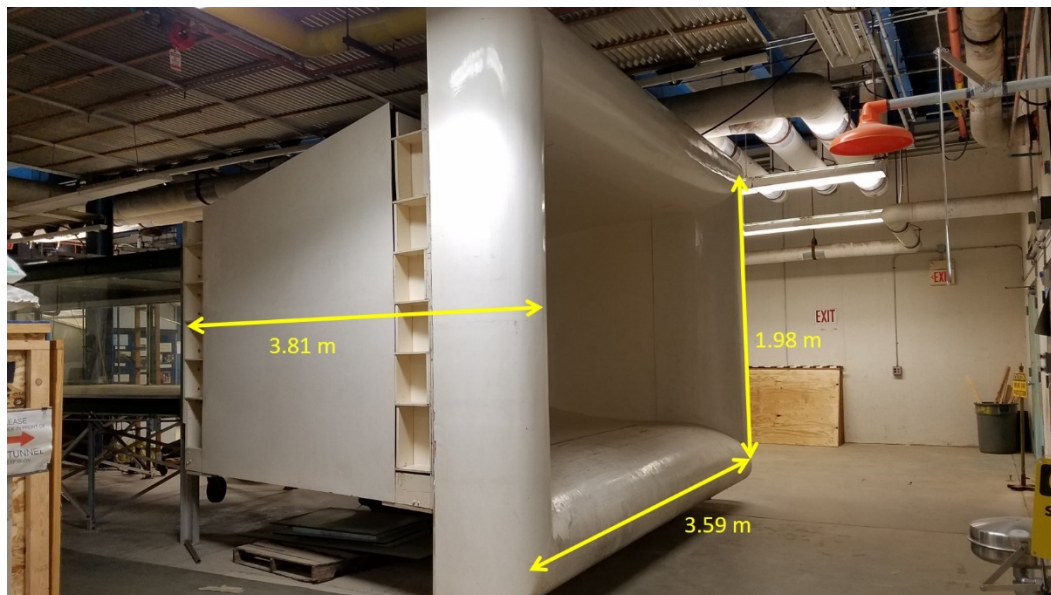


Figure 4. Inner dimensions of the contraction cone of the CRREL EWT.



### 2.1.2 Test section

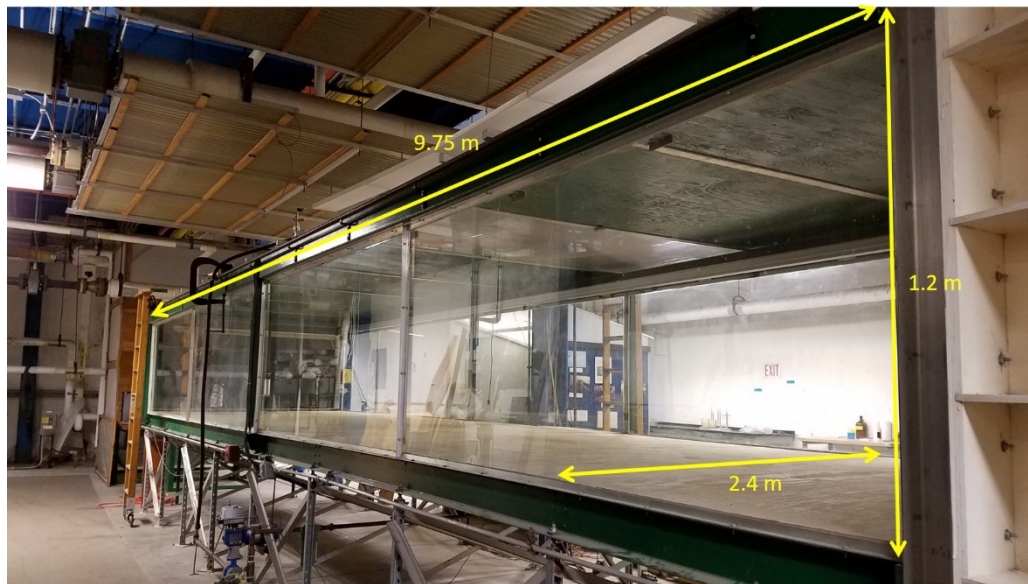
The size of the test section, or working section, of a wind tunnel depends on the quality of flow needed to perform experiments and to examine models of interest. Ultimately, there should be enough height and width within the section to keep wall effects from interfering with the flow around the test object (Bradshaw and Pankhurst 1964). The length of the working section in an atmospheric wind tunnel should be sufficiently long enough to grow a boundary layer along the floor and to provide a properly scaled simulated ABL prior to reaching the experimental setup in the test section. Unlike an aerodynamic wind tunnel, turbulence is expected in the test section.

The EWT is designed such that the testing section is located far downstream of the contraction inlet to allow the simulated ABL to develop over the simulated snow medium upstream of the test section. In the upstream development section, a particle reservoir is placed for particles to be entrained by the flow to simulate a blowing snow condition. The development section is attached directly to the contraction section (Figure 5) with the same rectangular cross section of the exit frame (i.e., 2.4 m [7.81 ft] by 1.2 m [4 ft] in width and height, respectively) and measures 9.75 m (32 ft) in length. It is constructed from steel and aluminum framing, with tongue-and-groove plywood panels for flooring. Each panel has dimensions 1.2 m by 2.4 m by 2 cm (4 ft by 8 ft by 0.75 in.) and is secured to the frame with screws. The ceiling is constructed from the same size plywood panels as



the floor and rests on the aluminum frame of the test section. The ceiling panels are removable to provide access for experimental setup and instrumentation installment and may be exchanged for plexiglass panels for a top down view of the test section.

Figure 5. Working section of the CRREL wind tunnel, measuring 9.75 m (32 ft) in length, 2.4 m (8 ft) wide, and 1.2 m (4 ft) tall; tempered glass siding provides an unobstructed view of the experimental setup.



The walls are constructed from several 2.4 m (8 ft) wide tempered glass panels 6.35 mm (0.25 in.) thick, which are attached with a silicone sealant. The panels provide observation of the entire length of the test section. Before reaching the fan section, a particle trap 0.3 m (1 ft) wide and 0.6 m (2 ft) deep catches particles rolling along the tunnel floor.

#### 2.1.2.1 Carriage system

The working section includes traversing gear with the intent to provide versatility in taking measurements within the tunnel while minimizing the flow disturbance in the tunnel. The possible uses of the carriage include measuring velocity profiles (vertical and horizontal), simulated drift topography, surface roughness, boundary-layer thickness along the floor and wall, and the free-stream velocity.

The carriage frame was designed to be tucked up close to the ceiling to minimize impact on the bottom surface boundary layer where snow drifting is of interest. The carriage consists of square rails down the length (z-



direction) and across the span (x-direction) of the tunnel and is outfitted with high-precision linear positioners manufactured by Parker Hannifan (Figure 6). The vertical rail (y-direction) is a slender, UniSlide, screw-actuated rail manufactured by Velmex.

Figure 6. The carriage system within the test section of the CRREL EWT.



The carriage controller system is constructed of several stepper motors and is controlled via LABVIEW virtual instrument (VI) software equipped with the motion toolbox. The VI can also support data acquisition for compatible instrumentation. Table 3 lists the range of motion characteristics from the right to left wall (+X), top to bottom (+Y), and contraction cone to fan (+Z). Instrumentation can either be mounted on the vertical rail or mounted directly to the steel frame of the carriage.

Table 3. The range of motion of the carriage system within the test section; X is measured from the right tunnel wall (looking down the tunnel from contraction) towards the left, Y is measured from the topmost of the vertical rail towards the floor, and Z is measured from the end of the contraction cone towards the fan.

Range	X	Y	Z
Maximum distance	193 cm (76.25 in.)	118.1 cm (46.5 in.)	914.4 cm (360 in.)
Minimum distance	25.4 cm (10 in.)	53.3 cm (21 in.)	121.9 cm (48 in.)

### 2.1.3 Fan

Airflow is generated via suction in the EWT. The fan is a six-blade, shaft-driven system manufactured by Joy Technologies, Inc. (Figure 7a), and has a diameter of 1.14 m (45 in.). The system is a fixed-speed (1780 rpm) variable-pitch system powered by 460 V, and has a maximum volume flow of 29.7 m<sup>3</sup>/s (63,000 cfm). Flow is controlled by varying the blade pitch using a Simpson Hawk II digital panel meter. Rotational velocity in the airflow is reduced by the cross piece located within the contraction transition section (Figure 7b).

A short contracting passage connects the test section to the fan (Figure 7c). The 2.9 m<sup>2</sup> (31.25 ft<sup>2</sup>) rectangular cross-sectional area of the working section transitions to a 3.14 m<sup>2</sup> (11.04 ft<sup>2</sup>) circular cross section over a length of 2.7 m (8.9 ft). After the fan, the tunnel expands slightly to release airflow into the particle filter.

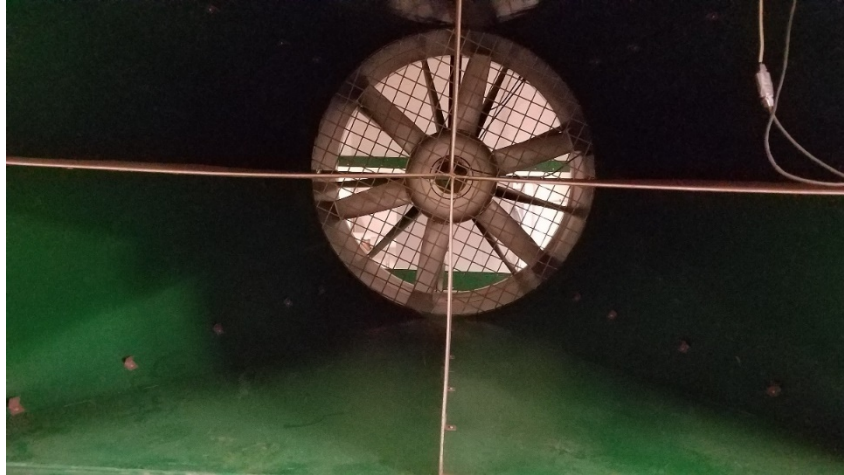
The acceleration of airflow through the contraction transition section should not have an impact on the airflow through the test section. Ear protection is recommended during use, especially when operating at maximum capacity (i.e., high blade pitch angle for maximum airflow).

### 2.1.4 Downstream trap

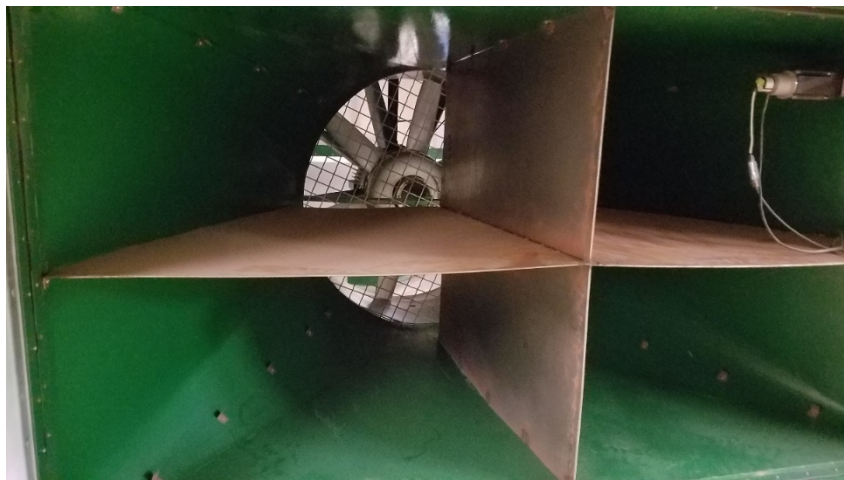
The physical modeling of snowdrifts requires the use of very fine particles to simulate snow. The tunnel was designed to collect these particles traveling both near the floor and through the air. The particle catch at the end of the test section is designed to capture material transported near the floor of the tunnel (Figure 8). The downstream trap, or particle filter, is designed to catch particles that were lifted into the flow high enough to be carried beyond the upwind floor trap.

Figure 7. (a) Front view of the fan (from the test section) with (b) a cross piece to reduce rotational velocity of airflow; (c) transition area between the test section and hopper, including particle trap, contraction transition, fan, and hopper.

(a)



(b)



(c)

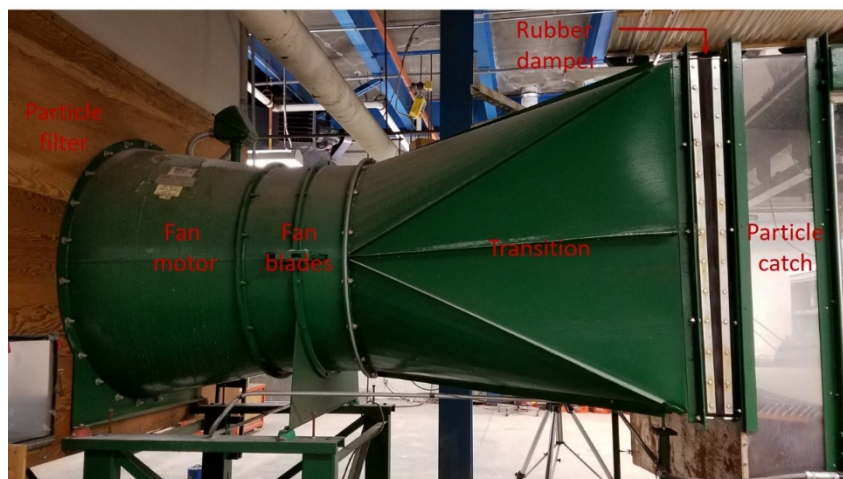
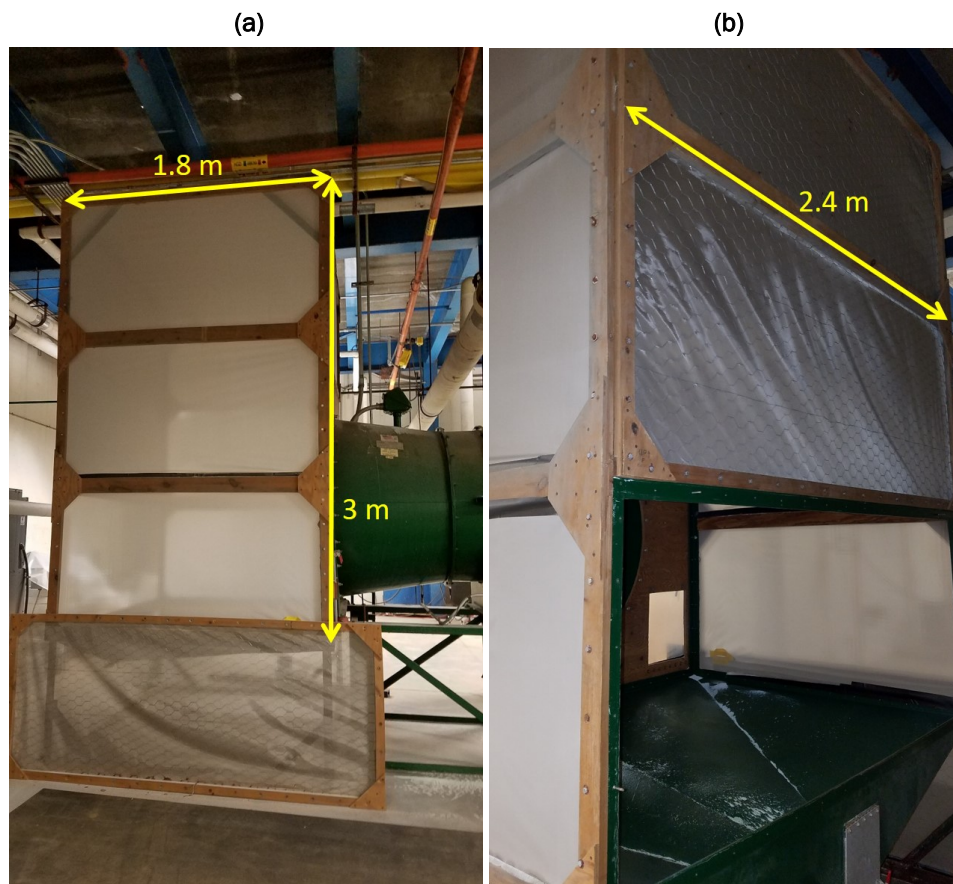


Figure 8. The downwind particle trap system located immediately after the fan of the CRREL EWT: (a) side view and (b) back view with lower back panel removed for access.



## 2.2 Instrumentation

The EWT is capable of supporting multiple sensors and instrumentation for a variety of experiments. The test section is currently equipped with a range-finding sensor, hot-wire anemometers, and Pitot tubes.

### 2.2.1 Range-finding sensor

The purpose of a laser range-finding sensor is to measure the simulated snow drift patterns made by a collection of fine particles around an experimental model. These sensors work by emitting a laser light source towards an object and detecting the return of the light reflected from the object's surface, thereby measuring the distance between the source and the reflecting surface.

Presently, an OMRON ZS-LD350S optical displacement sensor is installed on the vertical beam of the carriage system (Figure 9). The sensor uses a diffuse reflection optical system with a spot beam shape. In other words,



light is reflected in many directions from an object's surface (i.e., diffuse reflection), rather than in only a single direction (i.e., regular reflection), such that the sensor can detect a wider area of measurement. The spot beam shape allows for the accurate measurement of bumps or ripples in the object surface, rather than averaging the surface roughness (e.g., line beam). The sensor has a maximum measurement distance of 350 mm (13.7 in.)  $\pm$  135 mm (5.3 in.), using a semiconductor laser with wavelength 650 nm and a spatial resolution of 20  $\mu$ m.

Figure 9. OMRON ZS-LD350S displacement sensor located on the backside of the vertical beam of the carriage system in the test section of the EWT.



Recent efforts have looked at upgrading the displacement sensor from a spot beam profiler to a two-dimensional (2-D) laser profiler. A 2-D profiler would allow faster acquisition of the drift geometry as 2-D scans can be captured more quickly than taking point measurements of the same profile.

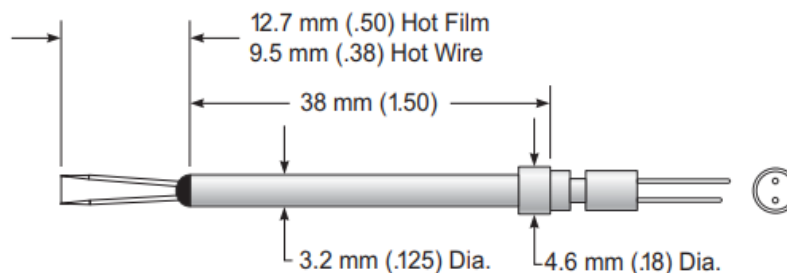
### 2.2.2 Hot-wire anemometer

As mentioned previously, a hot-wire anemometer is a type of thermal anemometer that maintains constant temperature across a very fine wire and measures the current required to maintain that temperature of the wire as cool air flows across it. That change in current is then related to the flow velocity. Hot-wire anemometers are ideal for turbulent flow applications as they have a high-frequency response to measure fluctuations in the flow (TSI Incorporated 2013).

The thermal anemometry system is operated by an IFA-300 Constant Temperature Anemometer (CTA) system with supporting computer software for control, data acquisition, and data analysis. The CTA is manufactured with eight channels, each capable of supporting measurements in one dimension (e.g., one channel is needed for X, one for Y, and one for Z). In other words, at least three channels are required when using a three-dimensional (3-D) probe. The CTA at CRREL has three channels installed currently; therefore, three one-dimensional (1-D) sensors can be read simultaneously (installed at different locations in the wind tunnel), or a single 3-D sensor can be installed to model the 3-D flow structure at a point in the wind tunnel.

Several models of TSI brand 1-D and 3-D hot-wire and hot-film anemometers are available for use in the EWT, allowing a wide range in frequency response and durability. The hot-film probes function the same as the hot-wire but are more durable in particulate flows, though their frequency response is poorer. Figure 10 shows an example of a 1-D general purpose device. Each device has a slightly different internal resistance, typically around 0.2 ohms. A number of extension rods and angle connectors are available to position the anemometer in-line with the air flow in different locations within the tunnel as needed. Each device is extremely delicate and should remain packed away when not in use.

Figure 10. Example of the TSI 1210 model general purpose 1-D hot-wire anemometer with dimensions shown in millimeters and inches (in parentheses); other model types can be found in TSI Incorporated (2013).



### 2.2.3 Pitot tube

Pitot tubes are typically used to measure air speed (e.g., of an aircraft). These devices measure the difference between static and dynamic pressure of airflow and relate it to flow velocity via Bernoulli's equation (Munson et al. 2006). The lower limit in velocity depends on the sensitivity of the pressure-sensing device. It can routinely measure velocities down to 0.25 m/s with a micromanometer or sensitive pressure sensor.

To reliably measure low differential pressures, a MKS Type 229 general purpose differential transmitter is connected to the Pitot tubes in the wind tunnel. Each tube is composed of a small cylinder with a hole down the axis of the tube connected to one side of the pressure transducer and several smaller holes around the circumference connected to the other side (Figure 11). The tube must be directed in-line with the airflow.

Figure 11. Example Pitot tube secured to the vertical rail of the carriage positioned in-line with the oncoming airflow.

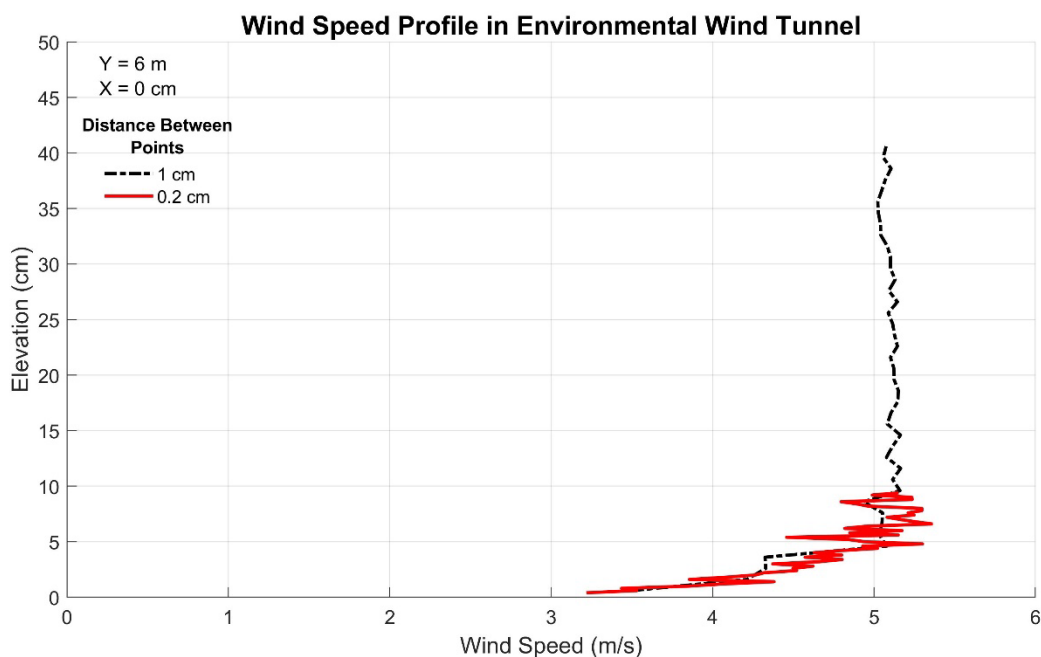


## 2.3 Velocity profile

The turbulence in the tunnel changes depending on what is on the floor of the tunnel. The flow field will behave differently over a smooth surface versus a dust- or particulate-covered surface or one with water or oil. The turbulent boundary layer may either need to be tripped to induce more turbulence early in the working section or smoothed to reduce the turbulence. These techniques depend on the physics and scaling of the desired model/experiment. It is recommended to perform a detailed flow-field analysis prior to experimentation to ensure that the physical modeling requirements are satisfied.

Haehnel et al. (1997) measured the velocity profile in the EWT (Figure 12) using a Pitot tube manometer over a sandy bed (i.e., glass beads). This profile was measured in the center of the test area of the working section near the fan, 6 m from the inlet of the working section. The flow field is characterized as a fully developed, neutrally stable turbulent boundary layer following equation (1).

Figure 12. Vertical velocity profile in the CRREL EWT





### **3 Recommendations for Expanded Capability**

#### **3.1 Modular test section**

The exchangeable test sections of the large European and German-Dutch wind-tunnel facilities (Boyet 2018) are aimed at expanding the capability to simulate different environments for various small- or full-scale models. For a smaller facility, such as at CRREL, an entirely replaceable test section is not feasible. Instead, the individual panels of the test section may be adapted to incorporate a variety of materials and structures in a modular manner at a relatively low cost. The objective of modularity in the wind tunnel is to harness the unique long, stable fetch characteristics to create a realistic simulation of turbulent conditions along a wide range of air-water and air-land surface interactions.

Currently, the tunnel is structurally built as a simple ladder frame in which a series of cross braces divide the bottom of the tunnel into “bays” between girders. The proposal is to build a truss frame below the test section to serve as the attachment point for an exchangeable test bed while also maintaining the rigidity of the structure. These test beds would be inserted from the side of the test section and positioned with levelling jacks to achieve the desired amount of exposure to wind, effectively replacing a section of plywood flooring with a different material or variable-height model.

The modular test section could entertain a variety of applications. A test bed of varying depth could contain materials ranging from vegetation to solid structures that could be progressively raised into the airflow. Tubs of water may be inserted to study air-water surface interactions with chemical slicks, such as oil dispersants and herders. The realism of dust patterns could be enhanced by controlling the entry layer (i.e., the height of the model surface tub) between continuous wind and the surface from which dust is generated.

#### **3.2 Exhaust control for hazardous materials**

The loss of the lysimeter wind tunnel from EL leaves a gap in the future study of air emissions from a bed of contaminated or hazardous organic materials. Presently, the use of some limited hazardous materials (e.g., oil) is possible in the EWT test section. In the case of other contaminants, such

as the dispersion of pollutants or chemicals from soil samples, the tunnel could be adapted to ventilate these air contaminants. A containment structure would be built in between the fan and hopper sections to collect contaminants within acceptable standards.

The exhaust would be regulated by repurposing the disused intake and exhaust fans from the ammonia refrigeration plant at CRREL and incorporating lever-controlled bypasses to supply makeup air and engage in high-rate exhaust from the containment structure. A filter assembly would be included to avoid exhaust entering the atmosphere. In combination with enhanced ventilation of the Ice Engineering Facility itself, the indoor space could be sufficiently ventilated and filtered by using readily available equipment at a relatively low cost for use with air contaminants.

### **3.3 Particle image velocimetry**

Particle image velocimetry (PIV) is a nonintrusive optical method to capture the instantaneous 2- and 3-D velocity field in airflow. In principle, particle-seeded flow (on the order of microns) is illuminated in a target area with a light sheet—typically from above. Two light pulses focused on the target area are recorded by a charged coupled device (CCD) camera where computer software then processes the movement of particles between the two frames into a representative velocity vector of the target area (Stanislas et al. 2000).

The ability to capture real-time velocity maps around models in the test section is invaluable in understanding the fluid dynamics of the experiment. With the addition of PIV to the wind tunnel, studies such as wind-driven airflow through a building (Lo 2014) would be possible at CRREL and could be adapted for cold regions research topics.

The necessary equipment and components (e.g., CCD cameras, lasers, light sheet optics, digital imaging software, and compatible computer) would be fairly expensive. However, the structure itself is primed to accept these components. The traversing system within the test section would be capable of supporting the light-sheet equipment with relatively low impact to the airflow. An external traversing system would be needed to support the CCD camera outside of the test section.

### 3.4 Cold capabilities

Refrigerated wind tunnels are common for aerodynamics purposes to study aircraft icing (e.g., NASA Glenn Research Center) (Addy and Chung 2000; Fortin and Perron 2009); however, they are rarely applied to study cold region dynamics. CRREL has a long history of successfully improvising equipment to function in a cold environment. In the case of the EWT, a new refrigeration system in the Ice Engineering Facility would allow construction of a room around the tunnel. This room would be large enough to have a “snow generation fetch” for snow guns to make real snow at the entrance of the wind tunnel. It would be powered by air-handler units from the central refrigeration system, and an agitator would present snow to the intake of the wind tunnel.

Rotating machinery and cold-temperature-vulnerable components would be replaced and hardened against wet operation. The filter would be modified to melt snow and recycle the water back to the snow-generation equipment (i.e., snow guns). It would be expected that the room could reach temperatures as low as  $-8.7^{\circ}\text{C}$  ( $-35^{\circ}\text{F}$ ). This modification would be the most expensive of the possible upgrades, costing up to \$1M or more but would also allow large-scale studies of organic icing and snow around structures.

## 4 Summary

ERDC has had an active presence in the field of research physical modeling with one historical, three operational, and one future atmospheric wind tunnel at EL, CRREL, and GSL. This report presented a high-level survey of the unique characteristics of the current ERDC wind-tunnel facilities. Though each tunnel is capable of generating turbulent flow conditions, they are each best suited for different applications. A recently decommissioned lysimeter wind tunnel at EL was in operation for 20 years to study the effect of air emissions from dredged material. At CRREL, the recirculating SDWT is ideal for small-scale snowdrift physical modeling while the EWT has historically been used for medium to large-scale snowdrift and particle entrainment modeling. The circular, open-return wind tunnel at GSL was designed for aerosol testing/sampling and particulate dispersion studies for DTRA. Table 4 summarizes the current and potential wind tunnel research applications available within ERDC.

These unique features mean that the operational wind tunnels within ERDC are ideal for recreating different atmospheric conditions. Of the three tunnels, the CRREL SDWT and EWT are able to explicitly recreate a turbulent boundary layer that can be modified slightly to meet the similitude requirements of individual experiments. The rectangular cross sections of the SDWT and EWT can accommodate multiple sensors within the working section while minimizing the effect of the instrumentation on the flow field. The GSL tunnel is primarily limited to installing instrumentation at or near the tunnel exit. The EWT is rather versatile in that the ceiling and floor panel can be removed or easily modified to accommodate other areas of interests, similar to the impinging jet studies (Haehnel et al. 2006, 2008; Haehnel 2008).

We provided a more detailed description of the physical structure, available instrumentation, and example velocity profile over a sandy bed for the CRREL EWT to document the present capability and identify potential areas of expanded capability. The tunnel measures a total of 12.3 m (60 ft) in length, consisting of a contraction section, transparent rectangular test section with a cross-sectional area of 2.9 m<sup>2</sup> (31.25 ft<sup>2</sup>), a particle trap, a suction fan, and particle filter components. It can support various instrumentation within the test section, including a displacement sensor, hot-wire anemometers, Pitot tubes, and more. The inner traversing gear pro-

vides versatility in measurement location. The tunnel is capable of achieving a turbulent flow velocity up to 11 m/s (36 ft/s) with a vertical velocity profile representative of a fully developed turbulent boundary layer.

There are several options for expanding the scope of the EWT modeling capability (Table 4). Few modifications are needed to exchange a portion of the uniform wooden floor with a modular test bed in the working section. Different materials (i.e., water, oil, or sand with or without vegetation) and model structures (e.g., solid wind-break model) could be inserted into the free stream with variable height, contributing to air-land and air-water interface research topics. Moderate adjustments to the exhaust and ventilation of the tunnel outflow would support the use of contaminated soils, such as dredge material, for pollutant dispersion studies. The addition of a PIV system to the tunnel would significantly enhance the ability to study complex fluid dynamics over and around a target area, largely contributing to the understanding of fluid flow processes in U.S. Army research areas. Lastly, the opportunity to modify the wind-tunnel components to withstand cold temperatures and establish a cold room around the tunnel is ideal to perform cold regions experiments (e.g. white-out snow conditions).

**Table 4. Current and potential research applications achievable by ERDC wind tunnel facilities.**

Research application	GSL	CRREL EWT	CRREL SDWT
Dispersion (aerosol / particulate)	✓	✓	
Dispersion (chemicals / pollutants)		❖	
Dust patter / lofting behavior		❖	
Flow visualization (e.g., smoke)		✓	
Meteorological sensor testing	✓	✓	
Oil herding		❖	
Snow drift modeling (lofting, entrainment, development around structures, etc.)		✓	✓
Wind resource assessment (terrain, vegetation, etc.)		❖	
Whiteout conditions (real snow)		❖	

❖ designates capabilities achieved with facility upgrade

ERDC has a suite of atmospheric physical modeling capabilities that offers a unique resource in support of the ERDC mission. Maintaining these capabilities, such that they continue to inform development of solutions to

present atmospheric challenges, and enhancing them in anticipation of future challenges promotes creative solutions. Further, this benefits our nation by providing a cost-effective resource that inspires development of novel methodologies to tackle tough problems.

## References

- Addy, H., Jr., and J. Chung. 2000. A wind tunnel study of icing effects on a natural laminar flow airfoil. In *Proceedings, 38th Aerospace Sciences Meeting and Exhibit*, 10–13 January, Reno, NV: Aerospace Sciences Meetings. <https://doi.org/10.2514/6.2000-95>.
- Anno, Y. 1986. Conversion of a low-speed wind tunnel to a snowdrift wind tunnel. *Cold Regions Science and Technology* 12:291–294.
- Baals, D. D., and W. R. Corliss. 1981. *Wind Tunnels of NASA*. Washington, DC: National Aeronautics and Space Administration.
- Blocken, B., J. Carmeliet, and T. Stathopoulos. 2007. CFD evaluation of wind speed conditions in passages between parallel buildings—effect of wall-function roughness modifications for the atmospheric boundary layer flow. *Journal of Wind Engineering and Industrial Aerodynamics* 95 (9–11): 941–962.
- Bocciolone, M., F. Cheli, R. Corradi, and G. Tomasini. 2008. Crosswind action on rail vehicles: Wind tunnel experimental analyses. *Journal of Wind Engineering and Industrial Aerodynamics* 96 (5): 584–610.
- Boyet, G. 2018. ESWIRP: European Strategic Wind tunnels Improved Research Potential Program overview. *CEAS Aeronautical Journal* 9 (2): 249–268.
- Bradshaw, P., and R. C. Pankhurst. 1964. The design of low-speed wind tunnels. *Progress in Aerospace Sciences* 5:1–69.
- Brown, S., and W. G. Nickling. 2008. A wind tunnel examination of shear stress partitioning for an assortment of surface roughness distributions. *Journal of Geophysical Research: Earth Surface* 113:F02S06. <https://doi.org/10.1029/2007JF000790>.
- Burri, K., C. Gromke, M. Lehning, and F. Graf. 2011. Aeolian sediment transport over vegetation canopies: A wind tunnel study with live plants. *Aeolian Research* 3 (2): 205–213.
- Cattafesta, L., C. Bahr, and J. Mathew. 2010. Fundamentals of wind-tunnel design. In *Encyclopedia of Aerospace Engineering*, ed. Richard Blockley and Wei Shyy. Hoboken, NJ: John Wiley & Sons, Ltd.
- Chong, T. P., P. F. Joseph, and P. O. A. L. Davies. 2009. Design and performance of an open jet wind tunnel for aero-acoustic measurement. *Applied Acoustics* 70 (4): 605–614.
- Clifton, A., J.-D. Rüedi, and M. Lehning. 2006. Snow saltation threshold measurements in a drifting-snow wind tunnel. *Journal of Glaciology* 52 (179): 585–596.
- Fortin, G., and J. Perron. 2009. Spinning rotor blade tests in icing wind tunnel. In *Proceedings, 1st AIAA Atmospheric and Space Environments Conference*, 22–25 June, San Antonio, TX.

- Graham, P. W., M. F. Cuddy, A. R. Poda, and G. E. Albritton. 2016. *Experimental Sampling Accuracy Results for Non-Explosive Wind Tunnel Tests Using Dry Particulate*. ERDC TR-16-12. Vicksburg, MS: U.S. Army Engineer Research and Development Center.
- Graham, P. W., S. C. Foster, G. E. Albritton, L. W. Stockham, and W. R. Seebaugh. 2011. *Experimental Results for the Accuracy of Mass Out-Flow Determined by Sampling*. ERDC/GSL TR-11-18. Vicksburg, MS: U.S. Army Engineer Research and Development Center.
- Haehnel, R. B. 2008. Physics of Particle Entrainment Under the Influence of an Impinging Jet. In *Proceedings, 26th Army Science Conference*, 1–4 December, Orlando, FL.
- Haehnel, R. B., and W. B. Dade. 2010. Particle entrainment by non-uniform eolian flow. In *Proceedings, ASCE Earth and Space Conference*, 14–17 March, Honolulu, HI.
- Haehnel, R. B., J. H. Wilkinson, and J. H. Lever. 1993. Snowdrift Modeling in the CRREL Wind Tunnel. In *Proceedings of the 50th Eastern Snow Conference*, 6–9 June, Quebec City, Quebec, 139–147.
- Haehnel, R. B., J. H. Lever, and R. D. Tabler. 1997. Field measurements of snowdrift development rate. In *Proceedings, 65th Western Snow Conference*, 4–8 May, Banff, Alberta.
- Haehnel, R. B., B. Cushman-Roisin, and W. B. Dade. 2006. Cratering by a subsonic jet impinging on a bed of loose particles. In *Proceedings, ASCE Earth and Space Conference*, 5–8 March, Houston, TX.
- Haehnel, R. B., W. B. Dade, and B. Cushman-Roisin. 2008. Crater evolution due to a jet impinging on a bed of loose particles. In *Proceedings, ASCE Earth and Space Conference*, 3–5 March, Long Beach, CA.
- Haehnel, R. B., T. U. Kaempfer, and M. A. Hopkins. 2010. A particle-scale model to simulation soil / regolith erosion. In *Proceedings, ASCE Earth and Space Conference*, 14–17 March, Honolulu, HI.
- Haehnel, R. B., N. Buck, and A. Song. 2014. Moisture effects on eolian particle entrainment. *Environmental Fluid Mechanics* 14:135–156.
- Kaimal, J. C., and J. J. Finnigan. 1994. *Atmospheric Boundary Layer Flows*. New York: Oxford University Press.
- Kanda, I., K. Uehara, Y. Yamao, and T. Marikawa. 2006. A wind-tunnel study on exhaust gas dispersion from road vehicles—Part I: Velocity and concentration fields behind single vehicles. *Journal of Wind Engineering and Industrial Aerodynamics* 94 (9): 639–658.
- Lever, J. H. 2000. Appendix E: Snowdrift model tests of NMD missile field at Ft. Greely, Alaska. In *Snow Characteristics at Fort Greely, Alaska for Testing the Silo Closure Mechanism*. ERDC/CRREL LR-01-36 (FOUO). Hanover, NH: U.S. Army Engineer Research and Development Center.



- Lever, J. H., and R. Haehnel. 1995. Scaling snowdrift development rate. *Hydrological Processes* 9:935–946.
- Lo, L. J. 2014. Particle image velocimetry experiments in a wind tunnel to study wind-driven airflow through building. In *Proceedings, 13th International Conference on Indoor Air Quality and Climate, Indoor Air 2014*, 7–12 July, Hong Kong.
- Munson, B., D. Young, and T. Okiishi. 2006. *Fundamentals of Fluid Mechanics*. New York: Wiley.
- NASA (National Aeronautics and Space Administration). 2015a. Open Return Wind Tunnel. Last modified 5 May 2015. <https://www.grc.nasa.gov/www/k-12/airplane/tunoret.html>.
- . 2015b. Closed Return Wind Tunnel. Last modified 5 May 2015. <https://www.grc.nasa.gov/www/k-12/airplane/tuncret.html>.
- Nieuwstadt, F. T. M., and P. G. Duynkerke. 1996. Turbulence in the atmospheric boundary layer. *Atmospheric Research* 40:111–142.
- Porte-Agel, F., Y.-T. Wu, H. Lu, and R. J. Conzemius. 2011. Large-eddy simulation of atmospheric boundary layer flow through wind turbines and wind farms. *Journal of Wind Engineering and Industrial Aerodynamics* 99 (4): 154–168.
- Scheiman, J. 1981. *Considerations for the Installation of Honeycomb and Screens to Reduce Wind-Tunnel Turbulence*. Technical Memorandum 81868. Hampton, VA: National Aeronautics and Space Administration, Langley Research Center.
- Schlichting, H., and K. Gersten. 2016. *Boundary-Layer Theory*. Berlin Heidelberg: Springer-Verlag.
- Song, A., and R. Haehnel. 2012. *Effects of Support Structure Porosity on the Drift Accumulation Surrounding an Elevated Building*. ERDC/CRREL TR-12-7. Hanover, NH: U.S. Army Engineer Research and Development Center.
- Stanislas, M., J. Kompenhas, and J. Westerweel. 2000. *Particle Image Velocimetry: Progress Towards Industrial Application*. Dordrecht, The Netherlands: Kluwer Academic Publishers.
- Thibodeaux, L. J., K. T. Valsaraj, R. Ravikrishna, K. Fountain, and C. Price. 2008. *Investigations of Controlling Factors for Air Emissions Associated with the Dredging of Indiana Harbor and Canal (IHC) and CDF Operations*. ERDC/EL TR-08-17. Vicksburg, MS: U.S. Army Engineer Research and Development Center.
- TSI Incorporated. 2013. *TSI Thermal Anemometry Probes Catalog*. Shoreview, MN: TSI Incorporated.
- White, F. M. 2015. *Fluid Mechanics*. 8th ed. New York: McGraw-Hill Education.

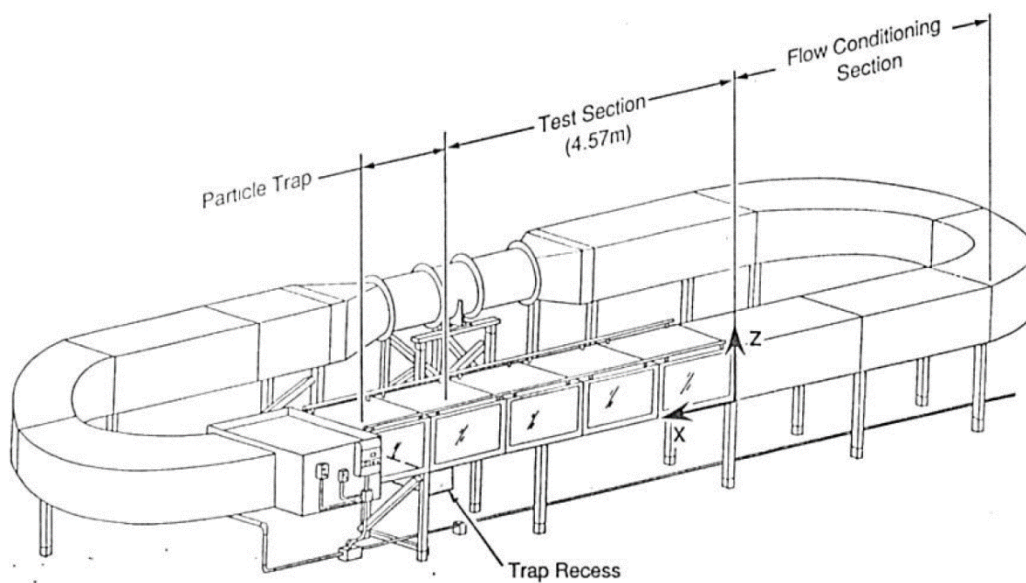
## Appendix A: Supplemental Information

This appendix provides supplemental schematics and velocity profile information for the CRREL recirculating wind tunnel and the GSL circular wind tunnel. While this is not comprehensive, it serves as a visual and complimentary aid to the material discussed in this report.

### A.1 CRREL SDWT

Remodeled from a low-speed wind tunnel, the Snow Drifting Wind Tunnel (SDWT) (Figure A-1) is a closed-return, recirculating tunnel that was later modified for improved snowdrift modeling capability.

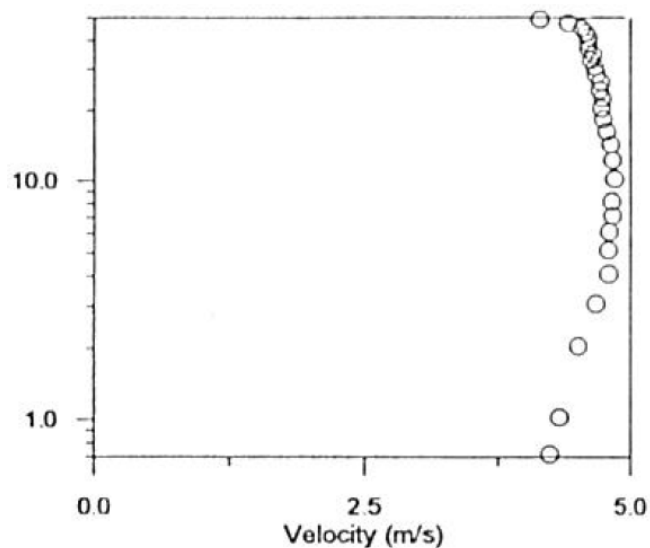
Figure A-1. Diagram of the CRREL Snow Drifting Wind Tunnel.



The SDWT has a rectangular cross section of  $0.46 \text{ m} \times 0.53 \text{ m}$  ( $1.5 \text{ ft} \times 1.7 \text{ ft}$ ) with a  $4.57 \text{ m}$  ( $15 \text{ ft}$ ) long test section. The test section was modified from its original design to be longer and was outfitted with glass panels for visibility. Wind speed can reach up to  $20 \text{ m/s}$  ( $45 \text{ mph}$ ) through the test section.

The vertical velocity profile in the SDWT is consistent with equation (1) and was shown to develop naturally over the simulated snow particles  $3 \text{ m}$  ( $9.8 \text{ ft}$ ) into the test section. The velocity follows a log-linear profile up to  $10 \text{ cm}$  ( $3.9 \text{ in.}$ ) from the tunnel floor (Figure A-2), which is adequate for the size of the tunnel.

Figure A-2. Experimental vertical velocity profile in the SDWT in the presence of drifting snow particles (e.g., glass beads).



## A.2 GSL Wind Tunnel

The GSL tunnel is a large, cylindrical tube 12.2 m (40 ft) in length with an inner diameter of 1.8 m (71.5 in.) and rests approximately 0.6 m (2 ft) above the ground on two cradle support structures (Figures A-3, A-4, A-5). Air flow is generated by a six-blade, high-volume, variable-speed industrial fan at the far end. An AC (alternating current) adjustable frequency drive is used to control the fan speed and can be set from 0 to 60 Hz at increments of 0.01 Hz (Graham et al. 2011).

Just downwind of the fan is a collection of PVC pipes (to correct fan-induced torque rotation) and a turbulence generation grid constructed of angle iron segments. The maximum exit flow velocity is 8.2 m/s (27 ft/s), with the inclusion of the PVC “baffle” (Graham et al. 2011). Installation of instrumentation is limited primarily to the mouth of the tunnel.

The tunnel velocity exit profile was measured to document the air flow characteristics. The nominal tunnel velocity was 4.5 m/s (10 mph) and was measured using an anemometer placed at four different radii along every 45° azimuth at the tunnel’s exit. Table A-1 shows the results.

Figure A-3. Cylindrical, open-return, push-down wind tunnel located at GSL in Vicksburg, MS.



Figure A-4. Side view diagram of the GSL wind tunnel (Graham et al. 2011).

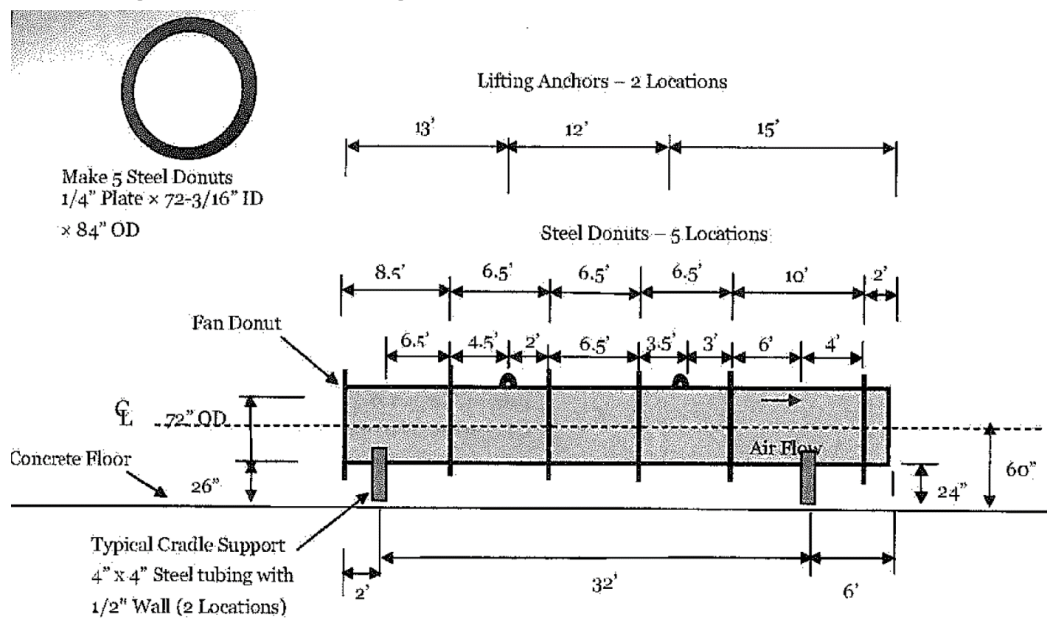


Figure A-5. Front view diagram of the GSL wind tunnel (Graham et al. 2011).

Note: 2 Cradle Supports Required: One Support (26" high) to be Placed at 12' from Inlet End of Tunnel and One Support (24" high) at 6' from Outlet

Approximate Total Weight of Tunnel, Fan, and all Steel Supports and Grid: 10,000 lb

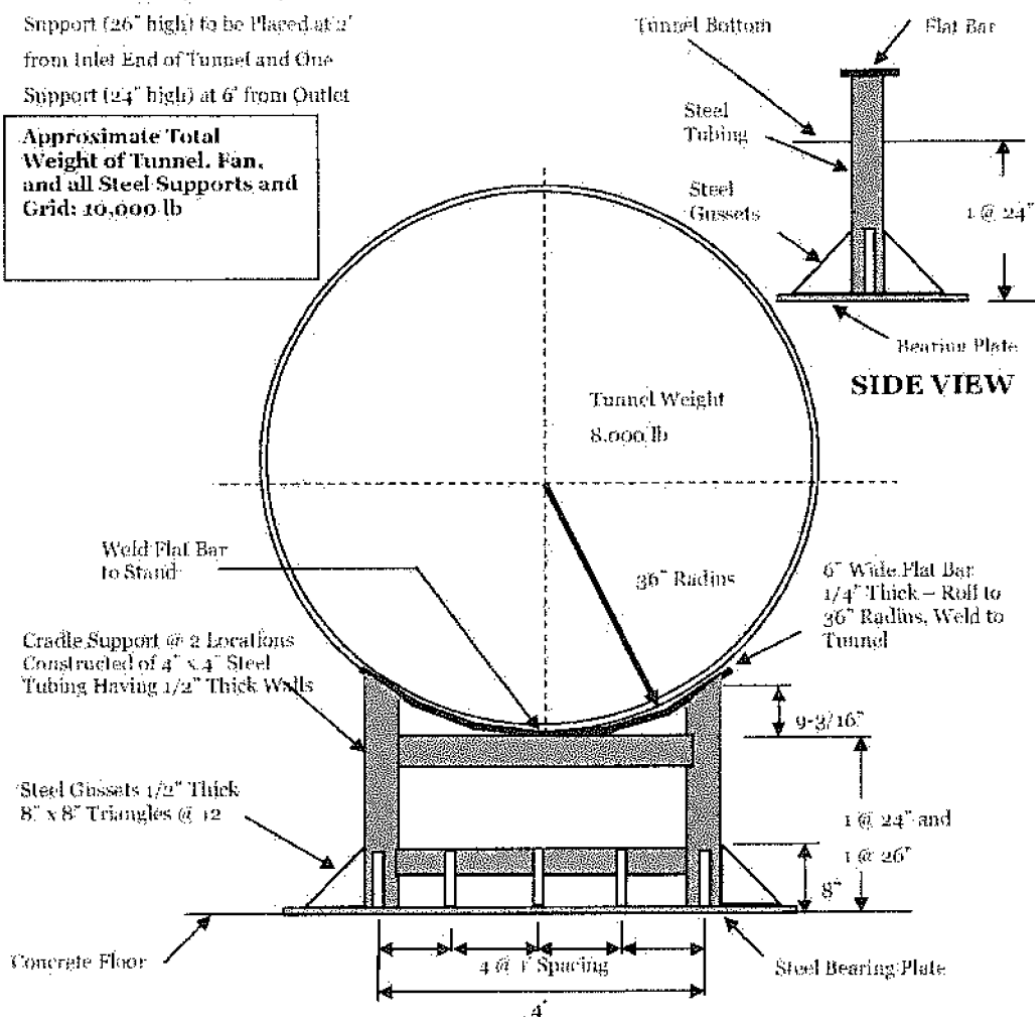


Table A-1. Measured tunnel exit velocity profile at a fan control of 32 Hz.

Measurement Along Radius (cm [ft])	Velocity in m/s (mph) at Location in Degrees							
	0	45	90	135	180	225	270	315
R = 0 (Center)	4 (9)	4.2 (9.4)	4.3 (9.6)	4.3 (9.5)	4 (9)	4.2 (9.4)	4.2 (9.4)	4.3 (9.6)
R = 30 (1.0)	4.1 (9.2)	4.3 (9.6)	4.4 (10)	4.6 (10.3)	4.4 (9.8)	4.3 (9.6)	4.3 (9.6)	4.3 (9.6)
R = 61 (2.0)*	4.1 (9)	4.6 (10.2)	4.6 (10.2)	4.8 (10.7)	4.6 (10.2)	4.4 (10)	4.6 (10.2)	4.4 (9.8)
R = 84 (2.75) (7 cm [3 in] from wall)	3.7 (8.3)	4.4 (9.9)	4.6 (10.3)	4.4 (9.9)	4.2 (9.4)	4.3 (9.5)	4.6 (10.2)	4.3 (9.4)

\*Nearest the sampler inlets at 67 cm (2.20 ft) radius.

# REPORT DOCUMENTATION PAGE

Form Approved  
OMB No. 0704-0188

Public reporting burden for this collection of information is estimated to average 1 hour per response, including the time for reviewing instructions, searching existing data sources, gathering and maintaining the data needed, and completing and reviewing this collection of information. Send comments regarding this burden estimate or any other aspect of this collection of information, including suggestions for reducing this burden to Department of Defense, Washington Headquarters Services, Directorate for Information Operations and Reports (0704-0188), 1215 Jefferson Davis Highway, Suite 1204, Arlington, VA 22202-4302. Respondents should be aware that notwithstanding any other provision of law, no person shall be subject to any penalty for failing to comply with a collection of information if it does not display a currently valid OMB control number. **PLEASE DO NOT RETURN YOUR FORM TO THE ABOVE ADDRESS.**

<b>1. REPORT DATE (DD-MM-YYYY)</b> May 2019			<b>2. REPORT TYPE</b> Special Report/Final		<b>3. DATES COVERED (From - To)</b>	
<b>4. TITLE AND SUBTITLE</b>  CRREL Environmental Wind Tunnel: Characteristics and Capabilities					<b>5a. CONTRACT NUMBER</b>	
					<b>5b. GRANT NUMBER</b>	
					<b>5c. PROGRAM ELEMENT NUMBER</b> 053HJ0/FAN U4357509	
<b>6. AUTHOR(S)</b>  Marissa J. Torres, Alexander R. Stott, Sandra L. LeGrand, and Marina Reilly-Collette					<b>5d. PROJECT NUMBER</b>	
					<b>5e. TASK NUMBER</b>	
					<b>5f. WORK UNIT NUMBER</b>	
<b>7. PERFORMING ORGANIZATION NAME(S) AND ADDRESS(ES)</b>  U.S. Army Engineer Research and Development Center (ERDC) Cold Regions Research and Engineering Laboratory (CRREL) 72 Lyme Road Hanover, NH 03755-1290					<b>8. PERFORMING ORGANIZATION REPORT NUMBER</b>  ERDC/CRREL SR-19-1	
<b>9. SPONSORING / MONITORING AGENCY NAME(S) AND ADDRESS(ES)</b>  Assistant Secretary of the Army for Acquisition, Logistics, and Technology 103 Army Pentagon Washington, DC 20314-1000					<b>10. SPONSOR/MONITOR'S ACRONYM(S)</b> ASA(ALT)	
					<b>11. SPONSOR/MONITOR'S REPORT NUMBER(S)</b>	
<b>12. DISTRIBUTION / AVAILABILITY STATEMENT</b> Approved for public release; distribution is unlimited.						
<b>13. SUPPLEMENTARY NOTES</b>  ERDC 6.2 Geospatial Research and Engineering (GRE) ARTEMIS STO-R DUST-CLOUD						
<b>14. ABSTRACT</b>  Atmospheric, or environmental, wind tunnels are ideal for basic research and applied physical modeling and for supporting the numerical model validation process. The U.S. Army Corps of Engineers, Engineer Research and Development Center (ERDC), has had an active presence in the field of research physical modeling. Between the ERDC Environmental Laboratory (EL), the Cold Regions Research and Engineering Laboratory (CRREL), and the Geotechnical and Structures Laboratory (GSL), there is one historical, three operational, and one future planned atmospheric wind tunnel. Each facility was uniquely designed to study different areas of atmospheric phenomena. This report reviews and highlights the characteristics of each facility and their target research applications. In particular, there is a desire to expand the scope of the CRREL Environmental Wind Tunnel (EWT) physical modeling capability. Expanding that capability beyond snowdrift modeling opens the door to geometrically full-scale turbulent-boundary-layer experiments on air-land and potentially air-water interfaces. Sustaining and improving internal wind-tunnel facilities is vital to the ERDC mission, promoting innovation and versatility in atmospheric physical modeling.						
<b>15. SUBJECT TERMS</b> Aerodynamics, Atmospheric physics, Atmospheric science, Scientific apparatus and instruments, Wind tunnels						
<b>16. SECURITY CLASSIFICATION OF:</b>				<b>17. LIMITATION OF ABSTRACT</b>  SAR	<b>18. NUMBER OF PAGES</b>  46	<b>19a. NAME OF RESPONSIBLE PERSON</b>
<b>a. REPORT</b>  Unclassified	<b>b. ABSTRACT</b>  Unclassified	<b>c. THIS PAGE</b>  Unclassified	<b>19b. TELEPHONE NUMBER</b> (include area code)			